ISSN 0020-1685, Inorganic Materials, 2008, Vol. 44, No. 3, pp. 272–277. © Pleiades Publishing, Ltd., 2008.
Original Russian Text © V.K. Ivanov, O.S. Polezhaeva, G.P. Kopitsa, A.E. Baranchikov, Yu.D. Tret'yakov, 2008, published in Neorganicheskie Materialy, 2008, Vol. 44, No. 3, pp. 324–330.

Fractal Structure of Ceria Nanopowders

V. K. Ivanov[a, b], O. S. Polezhaeva[a], G. P. Kopitsa[c], A. E. Baranchikov[a], and Yu. D. Tret'yakov[a, b]

[a] *Kurnakov Institute of General and Inorganic Chemistry, Russian Academy of Sciences, Leninskii pr. 31, Moscow, 119991 Russia*

[b] *Moscow State University, Vorob'evy gory 1, Moscow, 119899 Russia*

[c] *Konstantinov Institute of Nuclear Physics, Russian Academy of Sciences, Orlova Roshcha, Gatchina, Leningrad oblast, 188300 Russia*

e-mail: van@igic.ras.ru

Received May 22, 2007

Abstract—The formation of ceria nanoparticles from water–alcohol solutions of cerium(III) nitrate has been studied by UV/VIS spectroscopy, low-temperature nitrogen adsorption measurements, x-ray diffraction, transmission electron microscopy, and thermal analysis, and the effect of high-temperature annealing on the fractal structure of the CeO_2 nanopowders has been examined.

DOI: 10.1134/S0020168508030114

INTRODUCTION

Cerium dioxide (CeO_2) and related materials are widely used as ionic conductors, catalysts, sensors, UV filters, etc. [1–5]. In particular, ceria is the basic component of advanced high-temperature solid oxide fuel cells and three-way catalysts for post-treating exhaust gases [6, 7]. CeO_2 was also proposed for biomedical applications: the introduction of trace amounts of ceria into a retina reduces the adverse effect of UV radiation on photoreceptor cells [8]. According to Vodungbo et al. [9], doped ceria is a magnetic semiconductor possessing ferromagnetic properties at room temperature.

In most of these applications, use is made of nanocrystalline ceria with controlled particle size, specific surface, and aggregation, which determine the structure-sensitive properties of the material. To date, a variety of approaches have been proposed for size and specific surface control [10, 11]. At the same time, quantitative description of the aggregation behavior of nanopowders continues to be a challenge, primarily because there are no generally accepted analysis methods.

Approaches based on fractal geometry are among the most promising ways of describing ensembles of aggregated particles [12, 13]. Indeed, the fractal dimension of clusters measures the degree of filling of space and, consequently, can be considered an integral characteristic of the micromorphology of disperse materials.

In view of this, the objective of this work was to develop a process for the preparation of nanocrystalline ceria with controlled specific surface and to study the effect of synthesis and heat-treatment conditions on the particle size and fractal dimension of the synthesized nanopowders.

EXPERIMENTAL

Nanocrystalline ceria was prepared by adding aqueous ammonia to water–alcohol solutions of $Ce(NO_3)_3$. The starting chemicals used were reagent-grade $Ce(NO_3)_3 \cdot 6H_2O$, analytical-grade isopropanol, and 3 M aqueous ammonia. 0.08 M cerium(III) nitrate solutions in water–isopropanol mixtures with water : alcohol volume ratios of 1 : 1, 1 : 3, 1 : 6, and 1 : 19 were rapidly added to vigorously stirred aqueous ammonia taken in fivefold excess. The reaction was then left standing at room temperature for 2 h. The resultant precipitates were washed three times with isopropanol, centrifuged, and dried at 60°C for 2 h. The samples obtained at water : alcohol volume ratios of 1 : 1 and 1 : 6 were then annealed at 200, 300, 400, 500, 600, and 700°C for 2 h.

During synthesis, we took aliquots (0.5 ml) of the CeO_2 suspensions and measured their transmission spectra in the UV/VIS spectral region. Since the absorbance of the solutions exceeded 1.5, the aliquots were diluted with distilled water (1 : 40 to 1 : 80).

Transmission spectra were measured on an SF-2000 single-beam spectrophotometer[1] in the range 190 to 1010 nm in 0.1-nm steps. The optical slit width was 0.2 nm. As the light source, we used a deuterium lamp in the range 190 to 394.5 nm and a halogen lamp between 395 and 1010 nm. The exposure time was

[1] OKB Spektr, Russia.

50 ms. For each sample, the results were averaged over ten scans.

The band gap of CeO_2 nanoparticles was determined using plots of α^2E^2 versus E^2, where α is the absorption coefficient, and E is the photon energy. The sloping portion of each plot was approximated by a straight line, and the band gap was determined as the intercept of the line with the abscissa.

X-ray diffraction (XRD) measurements were performed on a DRON-3M powder diffractometer (CuK_α radiation) at a scan rate of 1–2°θ/min. The phases present were identified using JCPDS PDF data. XRD data were also used to evaluate the size of coherently scattering domains (CSDs). To this end, we used the Scherrer formula,

$$d_{CSD} = \frac{\lambda}{\beta\cos\theta},$$

where $\lambda_{Cu} = 1.54178$ Å, and β is the intrinsic width of the 111 diffraction peak from CeO_2.

Microstructures were examined by transmission electron microscopy (TEM) on a Leo912 AB Omega operated at 100 kV. Before TEM examination, each specimen was placed on a polymer-coated copper grid 3.05 mm in diameter.

The specific surface of the CeO_2 powders was determined by low-temperature nitrogen adsorption measurements with a QuantaChrome Nova 4200B analyzer. The samples were outgassed in a dry box at 40°C in vacuum for 5 h. The sample surface was analyzed by a multipoint (28 points) Brunauer–Emmett–Teller (BET) method. The pore size distribution was inferred from nitrogen desorption isotherms using the Barrett–Joyner–Halenda method. The fractal characteristics of surfaces were analyzed by the Neimark–Kiselev method, in which the surface fractal dimension is calculated using measured adsorption isotherms [14, 15].

Thermal analysis (DTA + TG) was performed in air during heating to 1150°C at a rate of 5°C/min, using a Perkin-Elmer TG7 analyzer. The sample weight was ~30 mg.

RESULTS AND DISCUSSION

UV/VIS spectroscopy data (Fig. 1) demonstrate that, just after mixing water–isopropanol solutions of cerium(III) nitrate with aqueous ammonia, the absorption spectrum shows a band in the range 280–300 nm, characteristic of CeO_2. Thus, the forming cerium(III) hydroxide oxidizes to cerium(IV) almost instantaneously. At the same time, heat-flow calorimetry results [16] indicate that, after mixing together such solutions at 25–30°C, heat evolution continues for 100–140 min. It is, therefore, reasonable to assume that, holding the suspensions in the mother solution leads to gradual dehydration of Ce(IV) hydroxy compounds and CeO_2 crystallization.

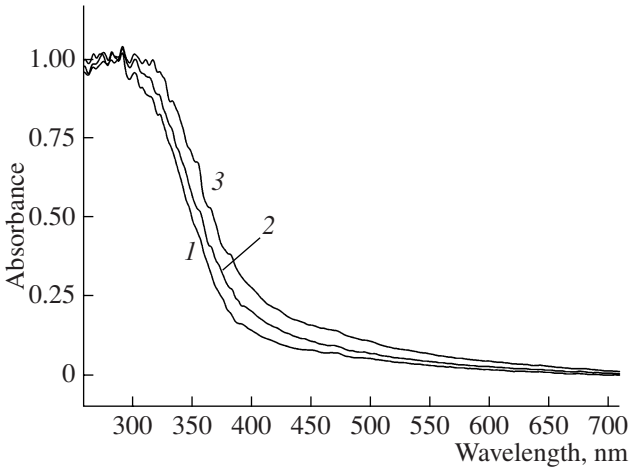

Fig. 1. UV/VIS absorption spectra of CeO_2 suspensions in water–isopropanol mixtures at synthesis times of (*1*) 5, (*2*) 20, and (*3*) 40 min.

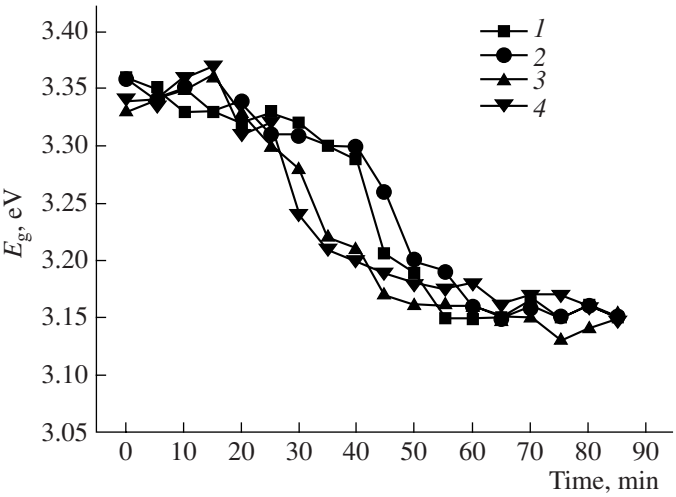

Fig. 2. Band gap of ceria as a function of synthesis time for solutions with water : isopropanol = (*1*) 1 : 1, (*2*) 1 : 3, (*3*) 1 : 6, and (*4*) 1 : 19.

Earlier calorimetry data [16] indicate that this process is autocatalytic: hydroxy complexes decompose predominantly on the surface of the CeO_2 particles formed, increasing their size. The same is evidenced by the UV/VIS spectroscopy data. Indeed, it follows from the data in Fig. 1 that, with increasing holding time, the absorption edge systematically shifts to longer wavelengths. The shift is due to the decrease in the band gap of the CeO_2 particles because of the reduction in the contribution of the quantum size effect.

Figure 2 shows the band gap of CeO_2, evaluated from UV spectroscopy data, as a function of the holding time of the suspensions in the mother solution. The band gap E_g is seen to gradually decrease from 3.35–

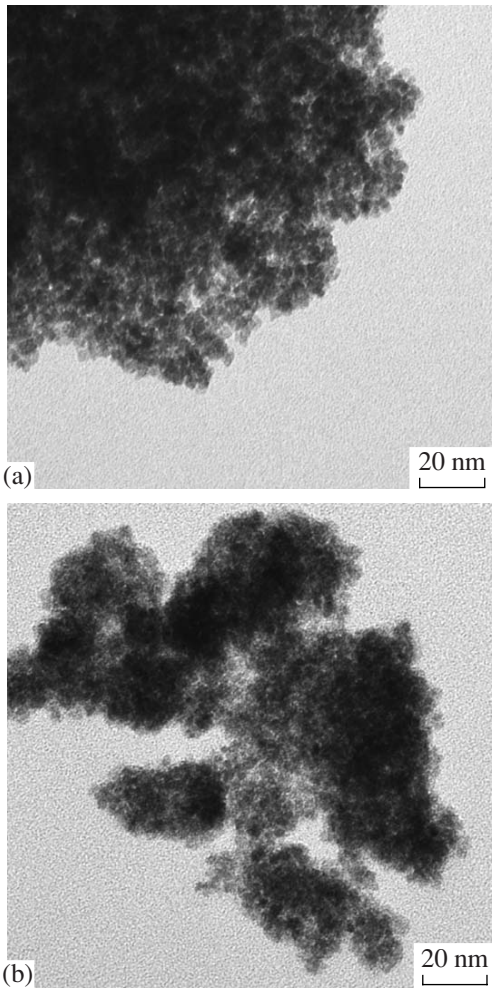

Fig. 3. TEM micrographs of ceria samples prepared from solutions with water : isopropanol = (a) 1 : 1 and (b) 1 : 19.

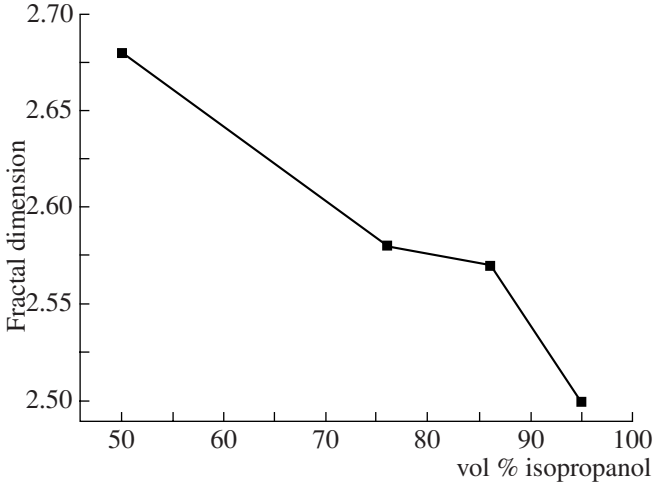

Fig. 4. CeO_2 surface fractal dimension as a function of initial isopropanol content.

3.40 to 3.15–3.20 eV. According to Zhang et al. [17], the initial E_g values are characteristic of CeO_2 particles 5.5–6.1 nm in diameter, while the final values are very close to the band gap of bulk ceria, E_g = 3.19 eV. Increasing the isopropanol content in the reaction system to 86–95% slightly reduces the growth time of the particles.

XRD results indicate the formation of cubic ceria (fluorite structure) with trace amounts of an amorphous phase (presumably, cerium hydroxy compounds). In all of the samples, the CSD size, evaluated from the width of the 111 peak, is ~5 nm. Thus, the isopropanol content in the reaction mixture has little or no effect on the size of the resulting CeO_2 particles. The same is evidenced by TEM data (Fig. 3): the samples prepared from the solutions with the lowest (50 vol %) and highest (95 vol %) isopropanol contents have the form of aggregated powders consisting of nearly monodisperse particles 4–5 nm in size. Note that the particle size evaluated from the UV/VIS spectroscopy data differs slightly from those determined by TEM and XRD, which is most likely due to aggregation of the CeO_2 nanoparticles.

According to the low-temperature nitrogen adsorption results, our samples range in porosity from 0.10 to 0.40 cm^3/g, with the largest contribution coming from micro- and mesopores more than 5 nm in size. The specific surface of the materials strongly depends on the solution composition: 220, 133, 124, and 110 m^2/g for the samples synthesized from the solutions containing 50, 75, 86, and 95% isopropanol, respectively. Neimark–Kiselev analysis of the nitrogen adsorption data indicates that, in the size range from 0.2 to 3.5 nm, all of the samples prepared by precipitation from water–alcohol solutions have fractal surfaces. Comparison with the CeO_2 particle sizes determined by TEM and XRD leads us to conclude that the fractal properties are due to the surface of the intergranular pores. Thus, it is reasonable to assume that fractal structures result from monomer–cluster or cluster–cluster aggregation of the nanoparticles.

This assumption is supported by the fact that the surface fractal dimension D depends on the isopropanol content of the water–alcohol mixtures (Fig. 4). It can be seen that, with increasing isopropanol content, D decreases systematically, which correlates well with the reduction in BET surface area. This attests to the formation of more compact aggregates, i.e., reducing the dielectric permittivity of the reaction mixture leads to a change in aggregation mechanism. Note also that the present experimental data are in conflict with the results reported by Chen and Chang [18], who found that the surface area of CeO_2 powders increased with increasing alcohol content in the reaction mixture. This is attributable to the effect of precipitation conditions on the aggregation behavior of nanoparticles.

According to the present thermal analysis data, obtained during heating in air, the TG curves of the

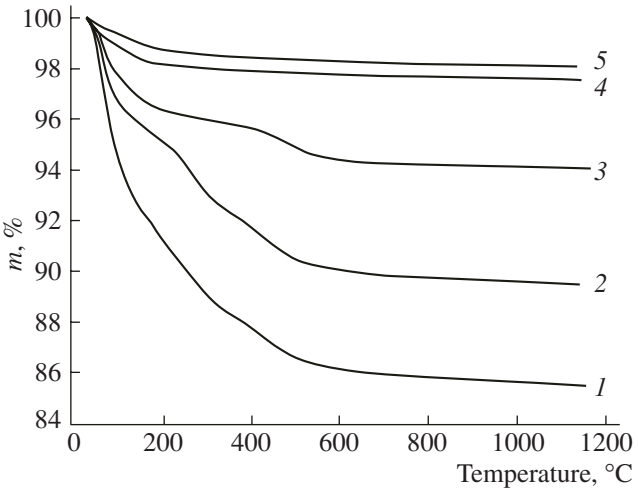

Fig. 5. TG curves of ceria samples prepared via precipitation from solutions with water : isopropanol = 1 : 1 and annealed at (*1*) 60, (*2*) 200, (*3*) 400, (*4*) 600, and (*5*) 700°C.

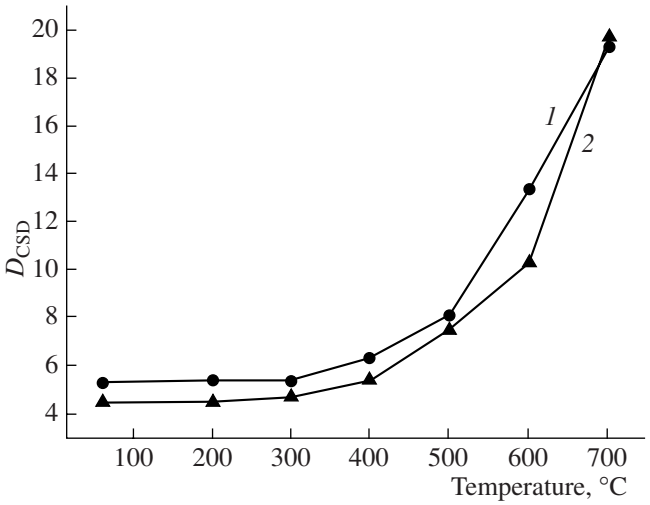

Fig. 6. CSD size as a function of annealing temperature for CeO_2 samples synthesized from solutions with water : isopropanol = (*1*) 1 : 1 and (*2*) 1 : 6.

CeO_2 samples prepared from different water–alcohol mixtures differ very little. The total weight loss is ≤15%. In the range 25 to 100°C, the samples loose adsorbed water, which is an endothermic process. As the temperature is raised to 200–250°C, the DTA curves show two reproducible, well-defined exothermic peaks, which are probably due to the crystallization of the amorphous component and the oxidation of the residual Ce(III). At higher temperatures, no thermal events were detected.

Note that the weight loss continues up to 1150°C. The TG curves can be divided into two portions: 25 to ~400°C and ~400 to 1150°C. The first portion corresponds to the release of chemically bonded and sorbed water; the nature of the higher temperature process is not yet fully clear. The most likely process is the removal of the residual bonded water, which only reaches completion at very high temperatures, like in the case of $ZrO_2 \cdot H_2O$ dehydration [19]. At the same time, according to Kim et al. [20], the surface layer of ceria nanoparticles is typically oxygen-deficient, and the deviation from stoichiometry increases markedly as the temperature is raised from 350 to 475°C. Therefore, the weight loss at temperatures from 400 to 1150°C may also be due in part to oxygen release.

To analyze in detail the processes that take place during high-temperature heat treatment of CeO_2, we performed thermal analysis of the powders precipitated from 1 : 1 mixtures of water and isopropanol and then annealed for 1 h at 200, 400, 600, and 700°C. The TG curves of those samples are presented in Fig. 5. Preannealing at 200 and 400°C is seen to systematically reduce the weight loss in the first step of the process, corresponding to the removal of chemically bonded and sorbed water. Under these annealing conditions, dehydration does not reach completion, leading to a significant weight loss in the first step (up to 5–10%). The samples preannealed at 600–700°C are fully dehydrated below 160°C. Thus, we are led to conclude that the observed weight loss (1.5–2%) is due to the removal of the water adsorbed during storage and that the samples contained no chemically bonded water.

According to XRD data (Fig. 6), high-temperature annealing of the CeO_2 powders leads to gradual growth of the nanocrystallites. The particle size of the ceria samples synthesized at different isopropanol contents varies little at annealing temperatures below 500°C and rises steeply at higher annealing temperatures.

TEM data (Fig. 7) also indicate that the particles grow insignificantly at low annealing temperatures.

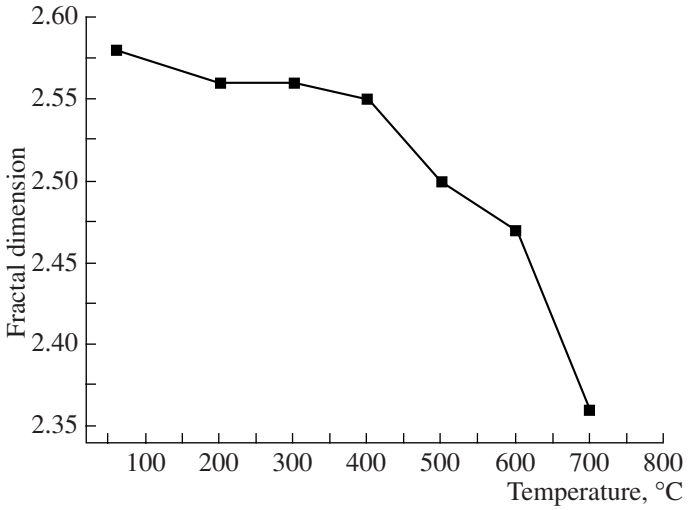

Fig. 7. CeO_2 surface fractal dimension as a function of annealing temperature.

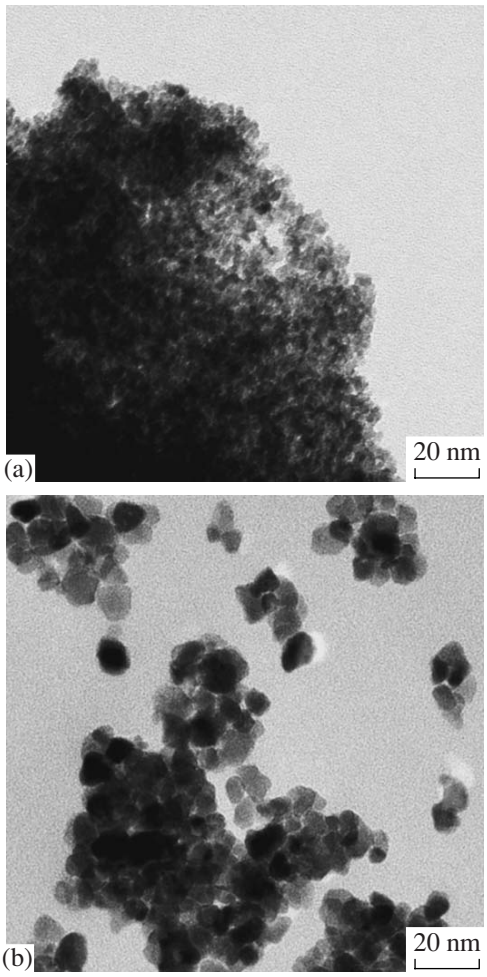

Fig. 8. TEM micrographs of ceria samples prepared from solutions with water : isopropanol = 1 : 1 and annealed at (a) 400 and (b) 600°C.

Note that annealing at 300–400°C leads to the formation of more regularly shaped particles in comparison with the unannealed samples, but the particle size distribution remains very narrow. In contrast, annealing in the range 500–700°C leads not only to marked particle growth (to ~20 nm) but also to a broader particle size distribution. According to low-temperature nitrogen adsorption data, the specific surface of the CeO_2 samples remains rather large (>100 m^2/g) at annealing temperatures from 200 to 400°C and decreases largely above 500°C.

The particle size evaluated from the adsorption data under the assumption that the nanoparticles are spherical in shape is on average 3–5 nm larger than that determined by TEM and XRD, which is obviously due to nanoparticle aggregation. d_{BET} is linearly related to d_{CSD} ($R^2 = 0.9994$), with no inflections. This indicates that the aggregation behavior of the nanoparticles remains unchanged over the entire temperature range studied.

According to Neimark–Kiselev analysis results, the physicochemical processes that take place during heat treatment of CeO_2 nanopowders, including the removal of chemically bonded and sorbed water and gradual recrystallization of the nanoparticles, do not lead to disappearance of the fractal structure of the sample surface. The boundaries of the self-similarity range also remain unchanged (0.2–3.5 nm), but the surface fractal dimension decreases systematically (Fig. 8). This finding correlates well with the observed effect of high-temperature annealing on the fractal structure of the surface of fine iron(III) oxide powders [21] and with other results [22, 23]. It is reasonable to assume that the reduction in fractal dimension on annealing, without disappearance of the fractal structure, is common to many systems and can be used to prepare fine-particle oxide materials of various compositions with controlled surface fractal dimension.

CONCLUSIONS

We studied the formation of nanocrystalline CeO_2 powders from water–alcohol solutions of cerium(III) nitrate. The results demonstrate that the solution composition has an insignificant effect on the size of the resulting CeO_2 particles but influences their aggregation behavior, specific surface, and surface fractal dimension.

We also studied the effect of annealing at temperatures from 200 to 700°C on the composition and micromorphology of the ceria powders. Our data indicate that high-temperature annealing can be used to control the surface fractal dimension of CeO_2 powders.

ACKNOWLEDGMENTS

We are grateful to the staff of the TsKP Prosvechivayushchaya elektronnaya mikroskopiya, Moscow State University, and especially to S.S. Abramchuk for studying the morphology of CeO_2 nanoparticles.

This work was supported by the Russian Foundation for Basic Research (project no. 08-03-00471), the Chemistry and Materials Science Division of the Russian Academy of Sciences (program no. 8), and the Presidium of the Russian Academy of Sciences (program no. 8).

REFERENCES

1. Fergus, J.W., Electrolytes for Solid Oxide Fuel Cells, *J. Power Sources,* 2006, vol. 162, pp. 30–40.
2. Yabe, S. and Sato, T., Cerium Oxide for Sunscreen Cosmetics, *J. Solid State Chem.*, 2003, vol. 171, pp. 7–11.
3. Izu, N. and Shin, W., Evaluation of Response Characteristics of Resistive Oxygen Sensors Based on Porous Cerium Oxide, *Sens. Actuators, B*, 2006, vol. 113, pp. 207–213.
4. Panzera, G., Modafferi, V., Candamano, S., et al., CO Selective Oxidation on Ceria-Supported Au Catalysts for

Fuel Cell Application, *J. Power Sources*, 2004, vol. 135, pp. 177–183.

5. Zerva, C. and Philippopoulos, C.J., Ceria Catalysts for Water Gas Shift Reaction: Influence of Preparation Method on Their Activity, *Appl. Catal.,* vol. 67, pp. 105–112.
6. Muraki, H. and Zhang, G., Design of Advanced Automotive Exhaust Catalysts, *Catal. Today,* 2000, vol. 63, pp. 337–345.
7. Gandhi, H.S., Graham, G.W., and McCabe, R.W., Automotive Exhaust Catalysis, *J. Catal.,* 2003, vol. 216, pp. 433–442.
8. Chen, J., Patil, S., Seal, S., and McGinnis, J.F., Rare Earth Nanoparticles Prevent Retinal Degeneration Induced by Intracellular Peroxides, *Nature Nanotechnol.*, 2006, vol. 1, pp. 142–150.
9. Vodungbo, B., Zheng, Y., Vidal, F., et al., Room Temperature Ferromagnetism of Co-Doped CeO_2 Diluted Magnetic Oxide: Effect of Oxygen and Anisotropy, *Appl. Phys. Lett.*, 2007, vol. 90, pp. 062 510.1–062 510.3.
10. *Binary Rare Earth Oxides*, Adachi, G. et al., Ed., Dordrecht: Kluwer, 2004.
11. *Catalysis by Ceria and Related Materials (Catalytic Science Series)*, Trovarelli, A., Ed., Singapore: World Scientific, 2002.
12. Harrison, A., *Fractals in Chemistry*, Oxford: Oxford Univ. Press, 1995.
13. Mandelbrot, B.B., *The Fractal Geometry of Nature,* New York: Freeman, 2000.
14. Neimark, A.V., Calculating Surface Fractal Dimension of Adsorbents, *Adsorpt. Sci. Technol.,* 1990, vol. 7, pp. 210–219.
15. Neimark, A.V., A Thermodynamic Approach for Calculating the Surface Fractal Dimension, *Pis'ma Zh. Eksp. Teor. Fiz.*, 1990, vol. 51, no. 10, pp. 535–538.
16. Ivanov, V.K., Sharikov, F.Yu., Polezhaeva, O.S., and Tret'yakov, Yu.D., Formation of Nanocrystalline Ceria from Water–Alcohol Solutions of Cerium(III) Nitrate, *Dokl. Akad. Nauk, Ser. Khim.,* 2006, vol. 411, no. 4, pp. 485–487.
17. Zhang, F., Jin, Q., and Chan, S.-W., Ceria Nanoparticles: Size, Size Distribution, and Shape, *J. Appl. Phys.*, 2004, vol. 95, pp. 4319–4326.
18. Chen, H.-I. and Chang, H.-Y., Homogeneous Precipitation of Cerium Dioxide Nanoparticles in Alcohol/Water Mixed Solvents, *Colloid. Surf. A: Physicochem. Eng. Aspects*, 2004, vol. 242, pp. 61–69.
19. Tarnopolsky, V.A., Aliev, A.D., Churagulov, B.R., et al., Influence of Thermal Treatment on the Ion Transport Properties of Hydrated Zirconia, *Solid State Ionics,* 2003, vols. 162–163, pp. 225–229.
20. Kim, S., Merkle, R., and Maier, J., Oxygen Non-stoichiometry of Nanosized Ceria Powder, *Surf. Sci.*, 2004, vol. 549, pp. 196–202.
21. Ivanov, V.K., Baranov, A.N., Oleinikov, N.N., and Tret'yakov, Yu.D., Synthesis of Ferric Oxide with Controlled Surface Fractal Dimension, *Zh. Neorg. Khim.*, 2002, vol. 47, no. 12, pp. 1925–1929.
22. Class, H.J. and de With, G., Fractal Characterization of the Compaction and Sintering of Ferrites, *J. Mater. Charact.*, 2001, vol. 47, pp. 27–37.
23. Beurroies, I., Duffours, L., Delord, P., et al., Fractal Geometry Change Induced by Compression Densification, *J. Non-Cryst. Solids,* 1998, vol. 241, pp. 38–44.